Proceedings of the 26th Chinese Control Conference
July 26-31, 2007, Zhangjiajie, Hunan, China

Design and Implementation of a Fully Autonomous Flight Control System for a UAV Helicopter*

Peng Kemao[1], Dong Miaobo[2], Chen Ben M.[2], Cai Guowei[2], Lum Kai Yew[1], Lee Tong H.[2]

1. Temasek Laboratories, National University of Singapore, Singapore 117508
E-mail: {kmpeng, kaiyew_lum}@nus.edu.sg

2. Dept of Electrical & Computer Engineering, National University of Singapore, Singapore 117576
E-mail: {eledm, bmchen, g0301341, eleleeth}@nus.edu.sg

Abstract: An autonomous flight control law applicable to full-envelope was designed in this manuscript for a small-scale unmanned aerial vehicle (UAV) helicopter to fly autonomously. The UAV helicopter was constructed based on a radio-controlled hobby helicopter by assembling an avionic system. The autonomous flight control law applicable to full-envelope was designed using a decentralized design methodology incorporating a newly developed nonlinear control techniques as well as dynamic inversion. The designed autonomous flight control law was implemented and verified in flight tests with the UAV helicopter. The flight test results demonstrate that the designed autonomous flight control law successfully drives the small-scale UAV helicopter to fly autonomously. The scheme of the autonomous flight control is applicable to flight control design of other UAVs.

Key Words: UAV Helicopters, Flight control, Nonlinear control, Decentralized control

1 INTRODUCTION

Unmanned aerial vehicles (UAVs) have recently aroused great interest in industrial and academic circles. Among the various types of UAVs, the small-scale UAV helicopter is the best one applied as typical plants for academic research as it is docilely manipulated in a manual mode and is easily operated in an automatic mode. The small-scale UAV helicopters are commonly upgraded from radio-controlled hobby helicopters by assembling an avionic system [1, 3, 6, 9]. The core issue, which is also one of challenges in the upgrading, is to design autonomous flight control laws which are able to drive the upgraded helicopters to fly autonomously.

Diverse methods had been explored to design autonomous flight control laws for small-scale UAV helicopters [5, 7, 8, 10]. The aim of the previous works was to realize autonomous flight of small-scale UAV helicopters. However, many of them were restricted in design of inner control laws and/or in a specific flight mode and the designed autonomous flight control laws were verified only in simulation. Therefore, there is much work left to be studied in designing autonomous flight control laws applicable to full-envelope and able to be verified in flight tests.

Autonomous flight control laws applicable to full-envelope consist of three portions: inner control law, outer control law and flight scheduling. and they are designed in the three portions respectively. Based on this scheme, an autonomous flight control law applicable to full-envelope is designed in this paper using a decentralized design methodology for a small-scale UAV helicopter. The decentralized design is a methodology to divide the plant into small portions for easy control design based on physical meaning. A newly developed nonlinear control technique, namely, the composite nonlinear feedback (CNF) control method [2, 4] is employed to design the inner control law based on the identified linear model of the UAV helicopter using in-flight data [1]. The dynamic inversion [5] is adopted to design the outer control law based on the kinematic models of the UAV helicopter in flight modes/missions. The flight scheduling is described in a discrete event system or " IF—THEN" to drive flight modes.

Fig. 1 The UAV helicopter, HeLion

The objectives of this manuscript are to design an autonomous flight control law applicable to full-envelope for a small-scale UAV helicopter and to verify feasibility of the designed autonomous flight control law and operability of the upgraded UAV helicopter in flight tests. A set of flight modes in the full-envelope are applied to verify operability of the upgraded UAV helicopter incorporating the designed autonomous flight control law in actual flight tests.

The UAV helicopter, HeLion, is upgraded from a radio-controlled hobby helicopter by assembling an avionic system [1]. A ground supporting system is built to support HeLion autonomous flight. HeLion is depicted in Fig. 1 and the schematic diagram of the operating system adopted in HeLion is shown in Fig. 2. The operating system in HeLion consists of the avionic system, ground supporting system and the manual operation system. The first two are to implement automatic operation and the last is kept as it is useful for modeling the UAV helicopter using in-flight data at the initial stage. Hence, HeLion is capable of operating in both the manual operation mode and the automatic control mode.

* This work is supported in part by Defence Science and Technology Agency (DSTA) of Singapore under a Temasek Young Investigator Award.

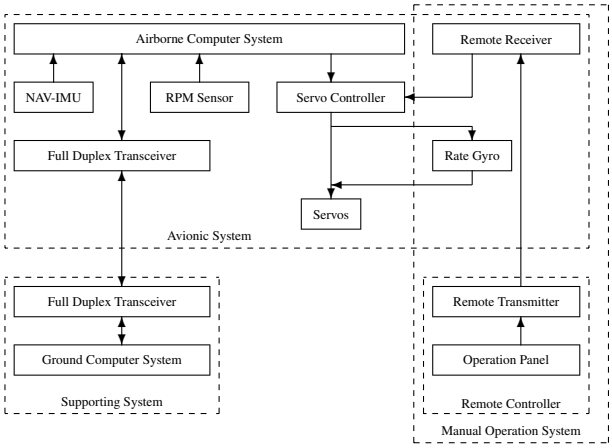

Fig. 2 Operating system adopted in HeLion

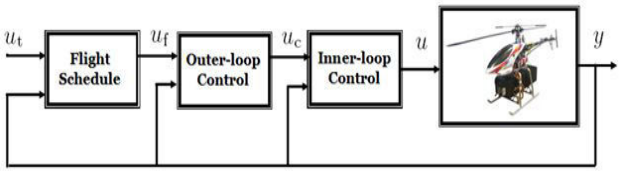

Fig. 3 Schematic diagram of a flight control system

In our UAV helicopter, HeLion, there are five servos in total. One servo is used to drive the ring engine is controlled by a governor to hold the spinning rate of the ring engine. Four others are be controlled for automatic flight. The measured signals are: ① three-axis acceleration; ② three-axis angular rates; ③ roll, pitch and yaw angles; ④ three-axis ground velocities; ⑤ longitude, latitude and local relative height. Note that Items 1, 2 and 4 are on the body frame.

2 FLIGHT CONTROL DESIGN

An autonomous flight control law can be divided into three portions, shown in Fig. 3, such as inner and outer control laws as well as flight scheduling. Based on the hierarchical structure, three loop systems are constructed such as the inner loop system composing of the inner control law and aircraft, outer loop system comprising the outer control law and the inner loop system, and the planning loop system where the flight scheduling is incorporated into the outer loop system. In Fig. 3, y is measurable outputs of the aircraft; u is the control signal to the aircraft produced by the inner control law; $u_{\rm c}$ is the command to the inner control law generated by the outer control law; $u_{\rm f}$ is the reference to the outer control law scheduled by the flight scheduling based on the flight missions, environment and external parameters.

The function of the inner loop system is to guarantee the asymptotic stability of the aircraft motion with respect to the surrounding air. The role of the outer loop system is to track the reference flight path and/or orientation of the aircraft scheduled by the flight scheduling. The task of the planning loop system is to pre-schedule and/or schedule the available reference flight path and/or orientation of the aircraft. The difference in one flight control system to another might be delimiters among the three portions, which do not affect functions of flight control systems.

Based on the schematic diagram of a flight control system, an autonomous flight control law applicable to full-envelope for our UAV helicopter, HeLion, comprises the inner control law, outer control law and flight scheduling. The function of the inner control law is to control $V_{\rm x}$, $V_{\rm y}$, $V_{\rm z}$ and ψ to track their references respectively. The role of the outer control law is to control $p_{\rm x}$, $p_{\rm y}$ and $p_{\rm z}$ to track their references respectively. The task of the flight scheduling is to preset a flight plan and generate the reference flight path subject to flight missions. The outer control design model is the displacement equation as follows,

$$\begin{pmatrix} \dot{p}_{\rm x} \\ \dot{p}_{\rm y} \\ \dot{p}_{\rm z} \end{pmatrix} = B'_{\rm b} \begin{pmatrix} V_{\rm x} \\ V_{\rm y} \\ V_{\rm z} \end{pmatrix} \tag{1}$$

where $B_{\rm b}$ is the transformation matrix from the NED frame to the body frame and is given by

$$B_{\rm b} = \begin{pmatrix} \cos\theta\cos\psi & \\ -\cos\phi\sin\psi + \sin\phi\sin\theta\cos\psi & \\ \sin\phi\sin\psi + \cos\phi\sin\theta\cos\psi & \\ \cos\theta\sin\psi & -\sin\theta \\ \cos\phi\cos\psi + \sin\phi\sin\theta\sin\psi & \sin\phi\cos\theta \\ -\sin\phi\cos\psi + \cos\phi\sin\theta\sin\psi & \cos\phi\cos\theta \end{pmatrix}$$

$V_{\rm x}, V_{\rm y}, V_{\rm z}$ are components of the ground velocity in meter per second in the body frame; ϕ, θ, ψ are the roll, pitch and yaw angles in radian respectively; $p_{\rm x}, p_{\rm y}, p_{\rm z}$ are components of the displacement in meter in the NED frame. The flight height $h = -p_{\rm z}$. The inner control design model is presented by augmenting the heading motion, $\dot{\psi} = \omega_{\rm z}$, into the identified linear model in [1] as follows,

$$\dot{x}_{\rm a} = A_{\rm a} x_{\rm a} + B_{\rm a} {\rm sat}(u) \tag{2}$$

where $x_{\rm a}$ and u are the state variable and control variable respectively as follows,

$$x_{\rm a} = (\, V_{\rm x} \;\; V_{\rm y} \;\; \phi \;\; \theta \;\; \omega_{\rm x} \;\; \omega_{\rm y} \;\; \tilde{a}_1 \;\; \tilde{b}_1 \;\; V_{\rm z} \;\; \psi \;\; \omega_{\rm z} \;\; w_{\rm zf} \,)'$$
$$u = (\, \tilde{\delta}_{\rm roll} \;\; \tilde{\delta}_{\rm pitch} \;\; \tilde{\delta}_{\rm col} \;\; \tilde{\delta}_{\rm pedal} \,)'$$

$\omega_{\rm x}, \omega_{\rm y}, \omega_{\rm z}$ are the roll pitch, yaw angular rates in radian per second respectively; a_1, b_1 are the first harmonics in radian of longitudinal and lateral flapping angles of the tip-path plane of the main blades respectively; $\delta_{\rm roll}, \delta_{\rm pitch}$ are the roll and pitch cyclic commands respectively; $\delta_{\rm col}$ is the collective command; $\delta_{\rm pedal}$ is the command of the tail rotor. All of commands are in $[-1, 1]$, where 1 and -1 in the first three elements of u denote $\frac{\pi}{4}$ rad and $-\frac{\pi}{4}$rad respectively; 1 and -1 in the last element of u denote $\frac{\pi}{4}$ rad/s and $-\frac{\pi}{4}$rad/s respectively. $\omega_{\rm zf}$ is a state variable of the filter associated with the original rate gyro in the manual operation system. Parameter with a $\tilde{\cdot}$, e.g., $\tilde{a}_1, \tilde{b}_1$ and $\tilde{\delta}_\star$, denotes a perturbed variable with respect to its hovering trim value.

All of state variables are measurable except $\tilde{a}_1, \tilde{b}_1$ and $\omega_{\rm zf}$. In the hovering state, trim values of all state variables are zero except a_1 and b_1, which are unknown and have no influence to the flight control design. The trim value of u in the hovering is as follows,

$$u_0 = [\, 0.05 \quad 0.02 \quad -0.22 \quad 0 \,]'$$

The spinning rate of the main blades is 1750rpm. The function sat is defined as follows,

$$\text{sat}(u_{\text{i}}) = \text{sgn}(u_{\text{i}}) \min\{|u_{\text{i}}|, \bar{u}_{\text{i}}\}, \qquad i = 1, 2, 3, 4.$$

with $\bar{u}_{\text{i}}$ being the saturation level of u_{i}.

$$\bar{u}_1 = 0.35, \;\; \bar{u}_2 = 0.35, \;\; \bar{u}_3 = 0.12, \;\; \bar{u}_4 = 0.4$$

The parametric matrices are given in convenience of decentralized design as follows,

$$A_{\text{a}} = \begin{bmatrix} \bar{A}_{11} & 0 \\ 0 & \bar{A}_{22} \end{bmatrix}, \;\; B_{\text{a}} = \begin{bmatrix} \bar{B}_{11} & 0 \\ 0 & \bar{B}_{22} \end{bmatrix}$$

$$\bar{A}_{11} = \begin{bmatrix} A_{11} & A_{12} & 0 & A_{14} \\ 0 & 0 & I_{2\times 2} & 0 \\ A_{31} & 0 & 0 & A_{34} \\ 0 & 0 & A_{43} & A_{44} \end{bmatrix}, \;\; \bar{B}_{11} = \begin{bmatrix} 0 \\ 0 \\ 0 \\ B_{41} \end{bmatrix}$$

$$\bar{A}_{22} = \begin{bmatrix} A_{55} & A_{56} & 0 \\ 0 & [0 \;\; 1] & 0 \\ A_{65} & A_{66} & A_{67} \\ 0 & A_{76} & A_{77} \end{bmatrix}, \;\; \bar{B}_{22} = \begin{bmatrix} B_{52} & 0 \\ 0 & 0 \\ B_{62} & B_{63} \\ 0 & 0 \end{bmatrix}$$

$$A_{11} = \begin{bmatrix} -0.1778 & 0 \\ 0 & -0.3104 \end{bmatrix}, \;\; A_{12} = \begin{bmatrix} 0 & -9.7807 \\ 9.7807 & 0 \end{bmatrix}$$
$$A_{14} = \begin{bmatrix} -9.7807 & 0 \\ 0 & 9.7807 \end{bmatrix}, \;\; A_{31} = \begin{bmatrix} -0.3326 & -0.5353 \\ 0.1903 & -0.2940 \end{bmatrix}$$
$$A_{34} = \begin{bmatrix} 75.7640 & 343.8600 \\ 172.6200 & -59.9580 \end{bmatrix}, \;\; A_{43} = \begin{bmatrix} 0 & -1 \\ -1 & 0 \end{bmatrix}$$
$$A_{44} = \begin{bmatrix} -8.1222 & 4.6535 \\ -0.0921 & -8.1222 \end{bmatrix}, \;\; B_{41} = \begin{bmatrix} 0.0496 & 2.6224 \\ 2.4928 & 0.1740 \end{bmatrix}$$
$$A_{55} = -0.6821, \;\; A_{56} = [0 \;\; -0.1070], \;\; B_{52} = 15.6491$$
$$A_{65} = -0.1446, \;\; A_{66} = (0 \;\; -5.5561)$$
$$A_{67} = -36.6740, B_{62} = 1.6349$$
$$B_{63} = -58.4053, \;\; A_{76} = [0 \;\; 2.7492], \;\; A_{77} = -11.1120$$

We proceed to design the flight control law in the sequence of the inner control law, the outer control law and the flight scheduling.

2.1 Design of Inner Control Law

The design model (2) for the inner control design is decoupled into two portions such as rolling, pitching portion and heaving, heading portion. The inner control law is designed in the two portions respectively using the decentralized design methodology incorporating the CNF control technique [4]. The rolling and pitching portion can be divided hierarchically into velocity, attitude and swashplate control design. The velocity and swashplate control design are completed using the pole placement and attitude control is designed with the CNF control method.

The control design for heaving and heading portion can be decoupled naturally. The heaving control is designed using the pole placement and the heading control is designed with the CNF control method. Note that there is an internal mode of ω_{zf} in the heading channel. Fortunately, dynamic of ω_{zf} is well asymptotically stable. It does not need to design a control law for it. However, we still need to design an observer to estimate it for the heading control.

The inner control law is given by

$$\begin{cases} \dot{x}_{\text{c}} = A_{\text{c}} x_{\text{c}} + B_{\text{c}} \begin{pmatrix} y_{\text{a}} \\ u \end{pmatrix} \\ \hat{x}_{\text{a}} = C_{\text{c}} \begin{pmatrix} x_{\text{c}} \\ y_{\text{a}} \end{pmatrix} \end{cases} \tag{3}$$

and

$$u = \begin{bmatrix} F_{\text{L1}} & 0 \\ 0 & F_{\text{L2}} \end{bmatrix} \hat{x}_{\text{a}} + \begin{bmatrix} G_{\text{L1}} & 0 \\ 0 & G_{\text{L2}} \end{bmatrix} \begin{pmatrix} V_{\text{x}} \\ V_{\text{y}} \\ V_{\text{z}} \\ \psi \end{pmatrix}_{\text{ref}} + \begin{bmatrix} M_1 & 0 \\ 0 & M_2 \end{bmatrix}$$
$$\times \rho \begin{bmatrix} N_1 & 0 \\ 0 & N_2 \end{bmatrix} \left\{ \begin{bmatrix} F_{\text{N1}} & 0 \\ 0 & I_{4\times 4} \end{bmatrix} \hat{x}_{\text{a}} - \begin{bmatrix} G_{\text{N1}} & 0 \\ 0 & G_{\text{N2}} \end{bmatrix} \begin{pmatrix} V_{\text{x}} \\ V_{\text{y}} \\ V_{\text{z}} \\ \psi \end{pmatrix}_{\text{ref}} \right\} \tag{4}$$

where x_{c} is the state variable of the observer and

$$y_{\text{a}} = (V_{\text{x}} \;\; V_{\text{y}} \;\; \phi \;\; \theta \;\; \omega_{\text{x}} \;\; \omega_{\text{y}} V_{\text{z}} \;\; \psi \;\; \omega_{\text{z}})'$$
$$\rho = \text{diag}\,(\rho_1 \;\; \rho_2 \;\; 0 \;\; \rho_4)'$$
$$\rho_1 = -\beta_1 \left| \tfrac{e^{-\alpha_1|\tilde{\phi}|} - e^{-1}}{1 - e^{-1}} \right|, \quad \rho_2 = -\beta_2 \left| \tfrac{e^{-\alpha_2|\tilde{\theta}|} - e^{-1}}{1 - e^{-1}} \right|$$
$$\begin{pmatrix} \tilde{\phi} \\ \tilde{\theta} \end{pmatrix} = \begin{pmatrix} \phi \\ \theta \end{pmatrix} - \left[F_{\text{ref}} \begin{pmatrix} V_{\text{x}} \\ V_{\text{y}} \end{pmatrix} + G_{\text{ref}} \begin{pmatrix} V_{\text{x}} \\ V_{\text{y}} \end{pmatrix}_{\text{ref}} \right]$$
$$\rho_4 = -\beta_4 \left| \tfrac{e^{-\alpha_4|\tilde{\psi}|} - e^{-1}}{1 - e^{-1}} \right|, \quad \tilde{\psi} = \psi - \psi_{\text{ref}}$$

The relevant parameters are presented as follows,

$$A_{\text{c}} = \begin{bmatrix} -13.1953 & 2.7138 & 0 \\ -3.7124 & -16.1191 & 0 \\ 0 & 0 & -14.7794 \end{bmatrix}$$

$$B_{\text{c}} = \begin{bmatrix} -0.0014 & 0.0127 & 0 & 0 & -0.0641 & -1.3027 \\ 0.0064 & 0.0163 & 0 & 0 & -1.4401 & -0.2540 \\ 0 & 0 & 0 & 0 & 0 & 0 \\ 0 & 0 & 0 & 0.0496 & 2.6224 & 0 & 0 \\ 0 & 0 & 0 & 2.4928 & 0.1740 & 0 & 0 \\ -0.0145 & 0 & 3.6715 & 0 & 0 & 0.1635 & -5.8405 \end{bmatrix}$$

$C_{\text{c}} =$

$$\begin{bmatrix} 0 & 0 & 0 & 1 & 0 & 0 & 0 & 0 & 0 & 0 & 0 & 0 \\ 0 & 0 & 0 & 0 & 1 & 0 & 0 & 0 & 0 & 0 & 0 & 0 \\ 0 & 0 & 0 & 0 & 0 & 1 & 0 & 0 & 0 & 0 & 0 & 0 \\ 0 & 0 & 0 & 0 & 0 & 0 & 1 & 0 & 0 & 0 & 0 & 0 \\ 0 & 0 & 0 & 0 & 0 & 0 & 0 & 1 & 0 & 0 & 0 & 0 \\ 0 & 0 & 0 & 0 & 0 & 0 & 0 & 0 & 1 & 0 & 0 & 0 \\ 1 & 0 & 0 & 0 & 0 & 0 & 0 & 0.01 & 0.025 & 0 & 0 & 0 \\ 0 & 1 & 0 & 0 & 0 & 0 & 0 & 0.025 & 0.01 & 0 & 0 & 0 \\ 0 & 0 & 0 & 0 & 0 & 0 & 0 & 0 & 0 & 1 & 0 & 0 \\ 0 & 0 & 0 & 0 & 0 & 0 & 0 & 0 & 0 & 0 & 1 & 0 \\ 0 & 0 & 0 & 0 & 0 & 0 & 0 & 0 & 0 & 0 & 0 & 1 \\ 0 & 0 & 1 & 0 & 0 & 0 & 0 & 0 & 0 & 0 & 0 & -0.1 \end{bmatrix}$$

$$F_{\text{L1}} = \begin{bmatrix} -0.0013 & -0.0601 & -0.5742 & 0.0479 & -0.0013 \\ 0.0726 & -0.0019 & -0.0733 & -0.6635 & -0.0352 \\ & & 0.0281 & -0.2605 & -3.4751 \\ & & -0.0169 & -1.2188 & -0.4924 \end{bmatrix}$$

$$G_{\text{L1}} = \begin{bmatrix} 0.0091 & 0.0855 \\ -0.0889 & 0.0103 \end{bmatrix}, \;\; G_{\text{L2}} = \begin{bmatrix} 0.0959 & 0 \\ 0.0027 & -0.0171 \end{bmatrix}$$

$$F_{\text{L2}} = \begin{bmatrix} -0.0523 & 0 & 0.0068 & 0 \\ -0.0039 & 0.0171 & -0.0847 & -0.6279 \end{bmatrix}$$

$$N_1 = \begin{bmatrix} 0.0051 & 0.0269 & 0.0013 & 0.0065 \\ 0.0435 & -0.0134 & 0.0092 & -0.0036 \end{bmatrix}$$

$$M_1 = \begin{bmatrix} 0.0810 & 6.8617 \\ 4.3195 & -1.3462 \end{bmatrix}$$

$$M_2 = \begin{bmatrix} 0 & 0 \\ 0 & 1 \end{bmatrix}, \quad N_2 = \begin{bmatrix} 0 & 0 & 0 & 0 \\ 0 & -0.0171 & -0.0285 & 0 \end{bmatrix}$$

$$F_{\text{N1}} = \begin{bmatrix} -0.0058 & -0.1182 & 1 & 0 & 0 & 0 & 0 & 0 \\ 0.1170 & -0.0012 & 0 & 1 & 0 & 0 & 0 & \\ 0 & 0 & 0 & 0 & 1 & 0 & 0 & 0 \\ 0 & 0 & 0 & 0 & 0 & 1 & 0 & 0 \end{bmatrix}$$

$$G_{\text{N1}} = \begin{bmatrix} 0.0047 & 0.1488 \\ -0.1345 & -0.0009 \\ 0 & 0 \\ 0 & 0 \end{bmatrix}, \quad G_{\text{N2}} = \begin{bmatrix} 0 & 0 \\ 0 & 1 \\ 0 & 0 \\ 0 & 0 \end{bmatrix}$$

$$F_{\text{ref}} = \begin{bmatrix} -0.0058 & -0.1182 \\ 0.1170 & -0.0012 \end{bmatrix},\ \alpha_1 = 0.1,\ \beta_1 = 1,\ \alpha_2 = 0.1$$

$$G_{\text{ref}} = \begin{bmatrix} 0.0047 & 0.1488 \\ -0.1345 & -0.0009 \end{bmatrix},\ \beta_2 = 0.6,\ \alpha_4 = 0.1,\ \beta_4 = 1$$

The relevant references are generated from the outer control law. The practical control signal to drive the helicopter comprises the dynamic control signal, u, by the inner control law, and the trim value of the hovering state, u_0, as follows,

$$u_{\text{P}} = u_0 + u \tag{5}$$

where u_{P} is the practical control signal. This completes the inner control design.

2.2 Design of Outer Control Law

The outer control law is designed according to the flight modes considered in the flight scheduling to generate the references to the inner control law. The scheduled flight modes need sufficient to represent available flight modes in full-envelope including steady and maneuvering flight. The scheduled flight modes are: 1) taking off; 2) hovering; 3) slithering; 4) head turning; 5) pirouette; 6) vertical turning; 7) spiral turning; 8) landing. The outer control law is mainly to control the velocity and/or position of the helicopter in the NED frame. The head direction of the helicopter is preset by the flight scheduling. The outer control law is designed based on the displacement equation (1) employing the dynamic inversion mode by mode.

2.2.1 Taking-off and Landing

A helicopter is taking off/landing in an ascending /descending speed, $\dot{h}_{\text{ref}}$, and holds a heading direction, ψ_{ref}, and the taking-off /landing point, $(\ p_{\text{x}} \quad p_{\text{y}}\ )'_{\text{ref}}$. The velocity reference is determined as follows,

$$\begin{pmatrix} V_{\text{x}} \\ V_{\text{y}} \\ V_{\text{z}} \end{pmatrix}_{\text{ref}} = \begin{pmatrix} \begin{pmatrix} \cos\psi & \sin\psi \\ -\sin\psi & \cos\psi \end{pmatrix} \begin{pmatrix} k_{\text{p}_{\text{x}}}(p_{\text{x}} - p_{\text{xref}}) \\ k_{\text{p}_{\text{y}}}(p_{\text{y}} - p_{\text{yref}}) \end{pmatrix} \\ -\dot{h}_{\text{ref}} \end{pmatrix} \tag{6}$$

where $k_{\text{p}_{\text{x}}}$ and $k_{\text{p}_{\text{y}}}$ are the feedback gains.

2.2.2 Hovering

Hovering means that a helicopter holds at a location at the NED frame, $(\ p_{\text{x}} \quad p_{\text{y}} \quad p_{\text{z}}\ )'_{\text{ref}}$, while holds its heading at a direction, ψ_{ref}. The velocity reference is determined as follows,

$$\begin{pmatrix} V_{\text{x}} \\ V_{\text{y}} \\ V_{\text{z}} \end{pmatrix}_{\text{ref}} = B_{\text{b}} \begin{pmatrix} k_{\text{p}_{\text{x}}}(p_{\text{x}} - p_{\text{xref}}) \\ k_{\text{p}_{\text{y}}}(p_{\text{y}} - p_{\text{yref}}) \\ k_{\text{p}_{\text{z}}}(p_{\text{z}} - p_{\text{zref}}) \end{pmatrix} \tag{7}$$

where $k_{\text{p}_{\text{z}}}$ is the feedback gain.

Tab. 1 Definition of events in flight scheduling

mode	description	transition condition	next mode
0	abnormal		2
1	taking-off	up to 15m high	2/0
2	hovering	a duration of 15s	3/9/A
3	slithering	a duration of 32s	4/0
4	turning back	a duration of 8s	5/0
5	head turning	a duration of 32s	6/0
6	pirouette	a duration of 32s	7/0
7	vertical turning	a duration of 62.8s	8/0
8	spiral turning	a duration of 40s	2/0
9	landing	on ground	A/0
A	termination		

2.2.3 Pirouette

Pirouette means that a helicopter turns in a spinning rate, $\dot{\psi}_{\text{ref}}$, a flight speed, V_{ref}, and a flight height, $h_{\text{ref}} = -p_{\text{zref}}$, while its head or tail is toward the center of its circular flight trajectory. The angle between the flight direction and the heading is $\pm\frac{\pi}{2}$ radians. The velocity reference is determined as follows,

$$\begin{pmatrix} V_{\text{x}} \\ V_{\text{y}} \\ V_{\text{z}} \end{pmatrix}_{\text{ref}} = V_{\text{ref}} \begin{pmatrix} 0 \\ \pm\cos\phi \\ \mp\sin\phi \end{pmatrix} + \begin{pmatrix} -\sin\theta \\ \sin\phi\cos\theta \\ \cos\phi\cos\theta \end{pmatrix} k_{\text{p}_{\text{z}}}(p_{\text{z}} - p_{\text{zref}}) \tag{8}$$

Due to space limitation, the other flight modes are skipped. The feedback gains in the outer control law are given as follows,

$$k_{p_{\text{x}}} = -0.3, \quad k_{p_{\text{y}}} = -0.3, \quad k_{p_{\text{z}}} = -0.5 \tag{9}$$

2.3 Design of Flight Scheduling

The flight scheduling is to preset an available flight path based on flight tasks and environmental parameters, and replan the flight path if any, to drive the UAV to complete flight missions. The flight scheduling can be described in a discrete event system or "IF—THEN" to organize flight modes. A practical flight scheduling for our UAV helicopter, HeLion, is designed in the event-driven model shown in Table 1. HeLion takes off, flies through the flight modes such as hovering, slithering, turning back, head turning, pirouette, vertical turning, spiral turning, hovering, and finally lands. In abnormal case, HeLion enters hovering state.

The complete autonomous flight control law for our UAV helicopter, HeLion, comprises the inner control law and outer control law as well as the flight scheduling.

3 FLIGHT TESTS

The designed autonomous flight control law is implemented to drive the UAV helicopter in actual flight tests, where the sampling period is 20ms. The target of the flight tests is to check operability of the UAV helicopter to autonomously complete flight missions with the designed autonomous flight control law. A set of flight modes is applied for the flight tests such as taking-off, hovering, slithering, turning

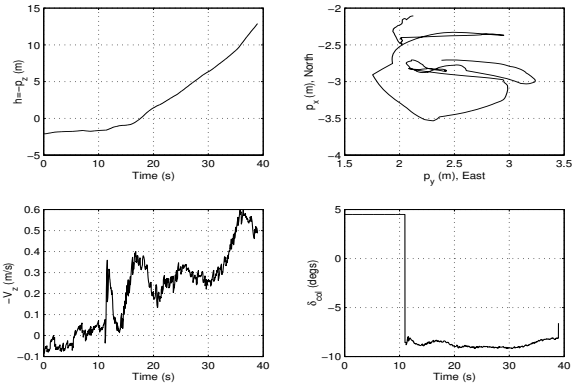

(a) Taking-off process

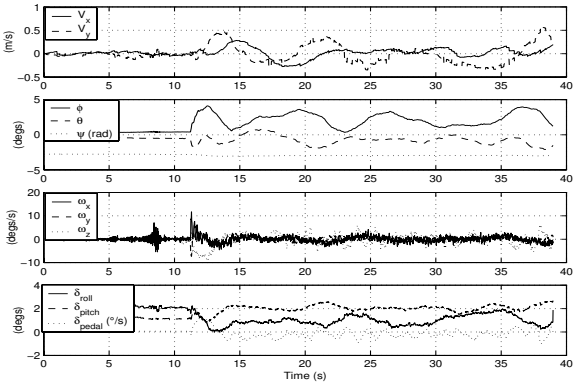

(b) Flight responses

Fig. 4 Flight mode: taking-off

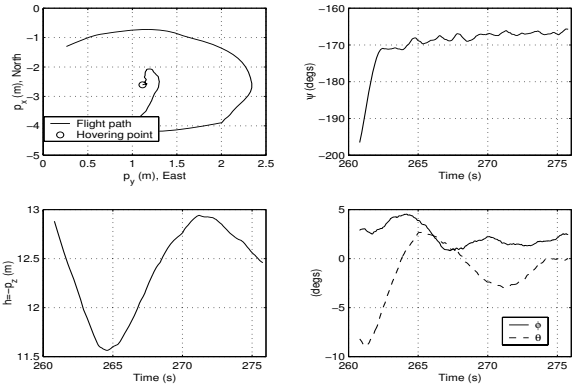

(a) Hovering process

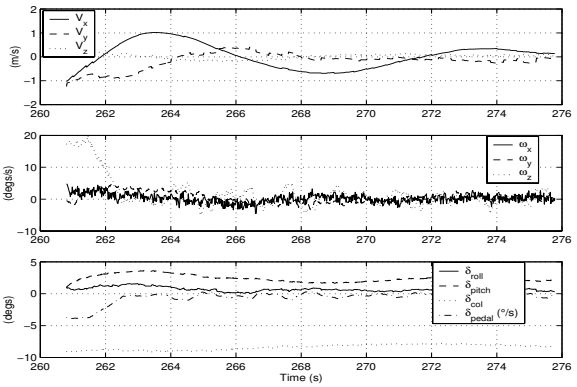

(b) Flight responses

Fig. 5 Flight mode: hovering

back, head turning, pirouette, vertical turning, spiral turning, hovering and landing. The flight results of the relevant flight modes are shown in Fig. 4 to 7.

The flight results in Fig. 4 to 7 demonstrate that the UAV helicopter with the designed autonomous flight control law successfully completes the flight mission consisting of a set of maneuvering and steady flight. The operability of the UAV helicopter is excellent in the flight test. However, the flight trajectory error is evident in the flight results. This is because of the adopted sensors in the avionic system. Note the displacement is measured by the GPS receiver whose resolution is $3\text{m}(\sigma)$. Taking this factor into consideration, the flight trajectory error is not too large. Another accurate sensor is adopted to measure the flight height to assist the taking-off/ landing when the UAV helicopter is near the ground. The range of the accurate sensor is no more than 1 meter, but its resolution is high up to 0.02 meters, The measured signal from the sensor is monitored when the UAV helicopter is flying in the flight height of 5 meters and applied in the flight control when it is effective.

4 CONCLUDING REMARKS

An autonomous flight control law applicable to full-envelope has been designed for our UAV helicopter, HeLion, with the decentralized design methodology incorporating the CNF control technique and the dynamic inversion. The designed autonomous flight control law has been successfully verified in various flight tests. Flight test results demonstrate that the UAV helicopter with the designed autonomous flight control law can autonomously finish a series of maneuvering

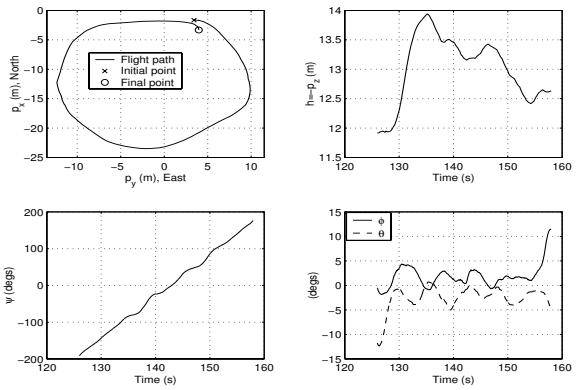

(a) Pirouette process

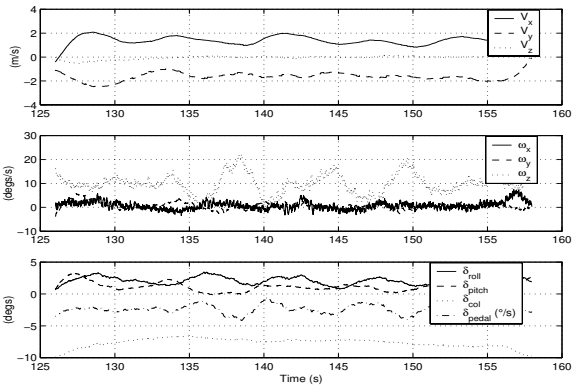

(b) Flight responses

Fig. 6 Flight mode: pirouette

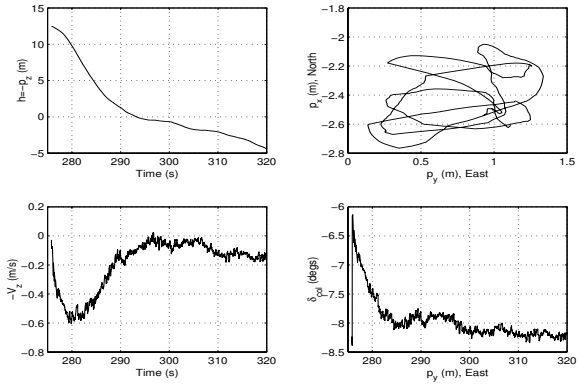

(a) Landing process

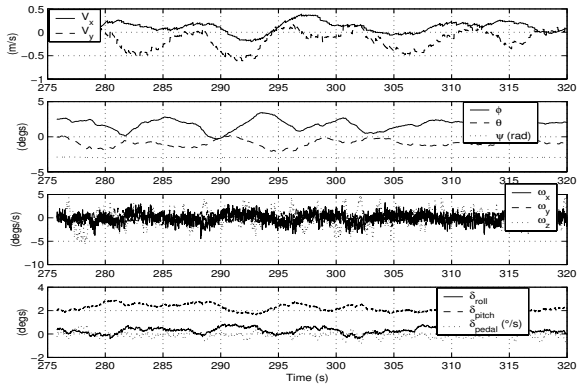

(b) Flight responses

Fig. 7 Flight mode: landing

and/or steady flight in its full-envelope including automatic taking off and landing. The operability of our UAV helicopter, HeLion, is excellent in flight tests. The scheme of the autonomous flight control is applicable to flight control design of other UAVs.

REFERENCES

[1] Cai G, Chen B M, Peng K, et al. Modeling and control system design for a UAV helicopter. Proceedings of the 14th Mediterranean Conference on Control and Automation, Ancona, Italy, WM1-4, 2006.

[2] Chen B M, Lee T H, Peng K, et al. Composite nonlinear feedback control for linear systems with input saturation: Theory and an application[J]. IEEE Transactions on Automatic Control, 2003, 48: 427-439.

[3] Gavrilets V, Shterenberg A, Dahleh M A, et al. Avionics system for a small unmanned helicopter performing aggressive maneuvers. Proceedings of the 19th Digital Avionics Systems Conferences, Philadelphia, USA, 2000.

[4] He Y, Chen B M, Wu C. Composite nonlinear control with state and measurement feedback for general multivariable systems with input saturation[J]. Systems & Control Letters, 2005, 54: 455-469.

[5] Isidori A, Marconi L, Serrani A. Robust nonlinear motion control of a helicopter[J]. IEEE Transactions on Automatic Control, 2003, 48: 413-426.

[6] Roberts J M, Corke P, Buskey G. Low-cost flight control system for a small autonomous helicopter. Proceedings of the 2002 Australian Conference on Robotics and Automation, Auckland, New Zealand, 2002.

[7] Shim D H, Kim H J, Sastry S. Control system design for rotorcraft-based unmanned aerial vehicle using time-domain system identification. Proceedings of the 2000 IEEE International Conference on Control Applications, Anchorage, Alaska, USA, 2000.

[8] Shim D H, Kim H J, Sastry S. Decentralized nonlinear model predictive control of multiple flying robots. Proceedings of the 42nd IEEE Conference on Decision and Control. Maui, Hawaii, USA, 2003.

[9] Sprague K, Gavrilets V, Dugail D, et al. Design and applications of an avionic system for a miniature acrobatic helicopter. Proceedings of the 20th Digital Avionics Systems Conferences, Daytona Beach, FL, USA, 2001.

[10] Sugeno M, Hirano I, Nakamura S, et al. Development of an intelligent unmanned helicopter. Proceedings of 1995 IEEE International Conference on Fuzzy Systems, Yokohama, Japan, 1995.